The Astrophysical Journal, 641: L145–L148, 2006 April 20

DEEP IMPACT: HIGH-RESOLUTION OPTICAL SPECTROSCOPY WITH THE ESO VLT AND THE KECK I TELESCOPE

E. Jehin,[1] J. Manfroid,[2] D. Hutsemékers,[2] A. L. Cochran,[3] C. Arpigny,[2]
W. M. Jackson,[4] H. Rauer,[5] R. Schulz,[6] and J.-M. Zucconi[7]
Received 2006 February 10; accepted 2006 March 10; published 2006 March 29

ABSTRACT

We report on observations of comet 9P/Tempel 1 carried out before, during, and after the NASA *Deep Impact* event (UT July 4), with the optical spectrometers UVES and HIRES mounted on the telescopes Kueyen of the ESO VLT (Chile) and Keck I on Mauna Kea (Hawaii), respectively. A total observing time of about 60 hr, distributed over 15 nights around the impact date, allowed us (1) to find a periodic variation of 1.709 ± 0.009 days in the CN and NH flux, explained by the presence of two major active regions; (2) to derive a lifetime $\gtrsim 5 \times 10^4$ s (at 1.5 AU) for the parent of the CN radical from a simple modeling of the CN light curve after the impact; (3) to follow the gas and dust spatial profiles' evolution during the 4 hr following the impact and derive the projected velocities (400 and 150 m s^{-1}, respectively); and (4) to show that the material released by the impact has the same carbon and nitrogen isotopic composition as the surface material ($^{12}C/^{13}C = 95 \pm 15$ and $^{14}N/^{15}N = 145 \pm 20$).

Subject headings: comets: general — comets: individual (9P/Tempel 1) — solar system: formation

Online material: color figures

1. OBSERVATIONS

High-resolution spectra of comet Tempel 1, the target of the NASA *Deep Impact* (*DI*) mission, have been collected with the UV-Visual Echelle Spectrograph (UVES) of the ESO VLT in early June (UT June 2, 7, and 8) and during a 10 night run around the *DI* event (UT July 2–11). The nights were photometric or clear, and the seeing excellent to good (0.4″–1.1″). Two long exposures (of ~7200 s) have been secured each night using two different beam splitters, a combination that allowed us to obtain on each observing date a spectrum covering the full optical range (304–1040 nm, except for a few narrow gaps). Both settings were chosen in order to include the CN (0–0) violet band near 388 nm. The narrow slit of the spectrograph (0.″44 × 10″ or 288 km × 6540 km on July 4) provides a resolving power $\lambda/\Delta\lambda \sim 83{,}000$ and was generally put on the center of light of the comet (and in a few cases at about 1.0″ from it). The position angle of the slit was along or perpendicular to the Sun-comet vector most of the time, and an atmospheric dispersion corrector (ADC) was used to sample the same region during a given exposure.

On July 4, the comet was setting at Paranal Observatory at the exact time of the *DI* event UT 05:52 (A'Hearn et al. 2005). The acquisition of the last UVES spectrum ended at UT 02:59, which was just a couple of hours before the impact, i.e., before the first spectrum obtained with HIRES, the High Resolution Echelle Spectrometer of the Keck I telescope installed on Mauna Kea (Hawaii). The comet was visible again from Paranal 17 hr later. The data sets are complementary: the UVES data set nicely describes the pre- and postimpact behavior of the comet, while the HIRES data set contains unique information about the direct consequences of the impact (up to 4 hr later).

The spectra have been reduced with special emphasis on the orders showing the CN band at 388 nm. We used the echelle package of the IRAF software (NOAO) to calibrate and extract the spectra. The dust-reflected sunlight underlying the cometary emissions was removed by subtracting a solar reference spectrum (the Moon, in this case) after the appropriate Doppler shift, profile fitting, and normalization were applied.

2. CN PERIODIC VARIATIONS

The relative flux in the CN band—between 386.2 and 387.5 nm and integrated over the full slit area—was calculated for the 13 nights of UVES observations.

The goal of the flux measurements was first to evaluate the variations triggered by the impact, but obvious flux variations of up to 30% were visible from night to night. A period search analysis has been performed using Fourier series fits and other methods like the Renson algorithm (Renson 1978) better suited for anharmonic light curves. It yielded a period of 1.709 ± 0.009 days (40.86 ± 0.05 hr) in very good agreement with the 1.701 ± 0.014 day rotation period determined from the *DI* spacecraft nucleus light curve (A'Hearn et al. 2005).

The phase diagram of the CN flux using this period is shown in Figure 1. The flux modulation is obviously synchronized with the rotation period and was stable over more than 1 month. The only deviating points are those corresponding to the first four postimpact measurements obtained on UT July 4 and 5 (phases around 0.45 and 0.1). There is no evidence of strong sporadic activity in the data. None of the 13 UVES observing dates correspond to the outbursts detected by the *DI* spacecraft or the ground-based observatories. After removing the periodic background, the light curve shows a net flux excess of about 20% and 7%, respectively, 17 and 41 hr after the impact, indicating that the gas released by the ejected material had not

[1] European Southern Observatory, Casilla 19001, Santiago, Chile; ejehin@eso.org.

[2] Institut d'Astrophysique et de Géophysique, Sart-Tilman, B-4000 Liège, Belgium; manfroid@astro.ulg.ac.be, hutsemekers@astro.ulg.ac.be, arpigny@astro.ulg.ac.be.

[3] Department of Astronomy and McDonald Observatory, University of Texas at Austin, C-1400, Austin; anita@barolo.as.utexas.edu.

[4] Department of Chemistry, University of California, 1 Shields Avenue, Davis, CA 95616; wmjackson@ucdavis.edu.

[5] Institute of Planetary Research, DLR, Rutherfordstrasse 2, 12489 Berlin, Germany; heike.rauer@dlr.de.

[6] ESA/RSSD, ESTEC, P.O. Box 299, NL-2200 AG Noordwijk, Netherlands; rschulz@rssd.esa.int.

[7] Observatoire de Besançon, 41 bis Avenue d'Observatorie, F-25010 Besançon Cedex, France; jmz@dalai-zebu.org.

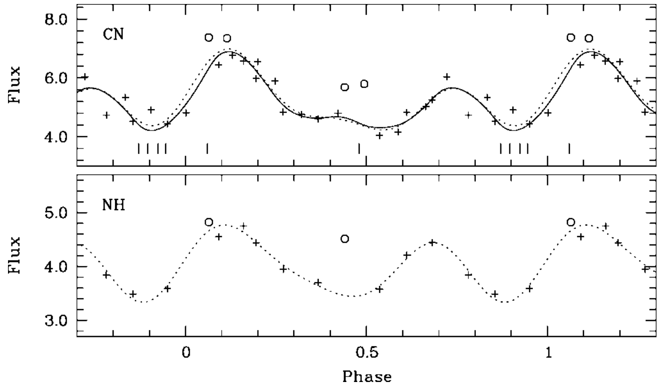

FIG. 1.—UVES CN and NH gas emission rotational phase diagrams. Zero phase is at the time of impact as observed from Earth: MJD 53,555.2445 (July 4, UT 05:52:02). In this figure, and in the following ones, the fluxes are given in arbitrary units. The dotted line models of the gas "light curves" are based on a three harmonic least-squares fit in which each data point has the same weight. The fit of the NH data is independent of the CN one, and the similarities of the two curves should be noted. Both data sets are phased to $P = 1.709$ days and reveal the existence of two main active regions. The observations can be accurately reproduced (*solid line*) with just three periodic bursts (or jets, corresponding to the observed bumps) starting to release gas at phases 0.25, 0.45, and 0.85 and with a duration of 8 hr (see text). The enhanced postimpact data for UT July 4 and 5 (around 23:00) are marked as circles and correspond to phases 0.44 and 0.49 and phases 0.06 and 0.11, respectively. The phase of the outbursts detected by the *DI* spacecraft are indicated as tick marks at the bottom of the figure. The scatter in the data comes from the centering and orientation of the slit, sky transparency, or intrinsic variability of the sources. The NH 0–0 (*A–X*) emissions at 336 nm appear only in the bluest setup, so we have only one data point per night for that species. [*See the electronic edition of the Journal for a color version of this figure.*]

yet completely vanished. After July 7.0 (and up to July 12.0), no excess could be detected at all in the region studied.

The shape of the CN phase diagram may be explained by the periodic passage of two major active regions, as well as a weaker one, into sunlight. Such an interpretation was also used to explain the comet Halley photometric observations during its 1985/1986 apparition (Schleicher et al. 1990). The brightest feature starts to produce gas around phase 0.9 (its minimum) and reaches its maximum (when the source stops its production) at phase 0.1. The second region is ∼20% less active and also lasts for about 8 hr (from phase 0.6 to phase 0.8). They could both be located at the same latitude (they see the Sun during the same amount of time), the difference in activity resulting from a different size or sunlight illumination of the active regions, for instance, due to different land morphology. The distance between the two features is a bit more than one-third of the rotation. The shoulder at phase ∼0.4 could be some evidence for the presence of a third and much fainter source.

The impact occurred at the beginning of the strongest periodic brightening (Fig. 1). It is then possible that this active region is visible close to the terminator in the images sent by the impactor. As already noted by A'Hearn et al. (2005), a possible candidate is the large and smooth area (labeled "a") in their Figure 1, and the scarp to the north of this feature would be an excellent candidate for a more localized, fast reacting region (the large smooth area being a kind of reservoir).

It is highly significant to note that almost all outbursts observed by the *DI* spacecraft (we have a precise knowledge of their onset time [A'Hearn et al. 2005]) correspond to minima in our gas-phase diagrams (see Fig. 1). Moreover four of the six outbursts are located just before the strongest brightening (phases from 0.85 to 0.95). Thus, the outbursts seem to be clearly associated with the active regions that we found (they occur at the same phases) and would be occasionally triggered when one of these regions comes into daylight. The outbursts could just be a particularly strong phase of outgassing from the same region.

The flux in the NH 0–0 (*A–X*) band at 336 nm shows a nice correlation with the CN variations, and any phase shift must be small, at most a couple of hours (Fig. 1). The first postimpact measurement has an excess of 30%, i.e., significantly more than CN, but, contrary to CN, the second one is not enhanced (or is only slightly enhanced), which means that NH disappeared sooner after the impact. Many more species are available in our spectra (OH, C_3, C_2, NH_2, etc.) and will be examined in the same way. This may provide us with interesting information on their respective parent lifetimes. For instance, the NH parent seems to have a similar lifetime to the CN parent lifetime because the phase shift between the two species is very small. With a lifetime in the range $(2–6) \times 10^4$ s (Wyckoff et al. 1988; Fink et al. 1991) for NH_2, similar to that of the CN parent [$(2–5) \times 10^4$ s; see Fray et al. 2005 and references therein], this observation is indeed in agreement with NH_2 being the main NH parent (Fink et al. 1991).

Data on HCN—a possible parent candidate of CN—have been obtained with the IRAM 30 m radio telescope from May 4.8 to 9.0 and show a 1.67 ± 0.07 day periodicity (Biver et al. 2005). The beam that was used sampled regions similar to those sampled by UVES (∼10″). The data have been phased with the 1.709 day period and superposed with the UVES CN flux measurements. There are only five HCN measurements, with large errors, so it is not possible to verify whether the differences we see in shape and phase with our CN light curve are real or not. If this is the case, this could be some additional evidence that HCN is not the only parent of CN (Fray et al. 2005; Manfroid et al. 2005).

3. CN AND DUST IMPACT LIGHT CURVES

Three preimpact spectra were obtained on May 30 with HIRES at the Keck I telescope, and a series of 14 relatively short exposures (10–30 minutes), with one right before the impact, were taken on the *DI* night.[8] The 0″.86 by 7″ slit provides a resolving power $\lambda/\Delta\lambda \sim 48,000$ and samples a comparable zone (563 km × 4578 km) to that of UVES. The slit was always centered on the nucleus and aligned along the parallactic angle. The weather was photometric on July 4, and the seeing excellent (∼0″.6).

The total CN flux in the slit has been calculated and normalized to the UVES fluxes by comparing the first preimpact spectrum of July 4 as well as the three May spectra with our derived light curve. The HIRES slit was 2 times wider than the UVES one and was always centered on the nucleus, leading to better measurement of the dust component. The consequences of the impact are readily seen in Figure 2, both in the dust and CN flux. The CN periodic variation has been removed using the UVES light curve, and the dust background has been taken out using the preimpact spectrum.

The total CN flux reaches its maximum at UT 07:28 (±10 minutes) or 5760 ± 600 s after the impact. It is enhanced by a factor of 2.8 compared with the preimpact situation. The decline is explained (at least partially) by the molecules starting to leave the slit area, mostly through the slit length (the lifetime

[8] Those data are publicly available at http://msc.caltech.edu/deepimpact/.

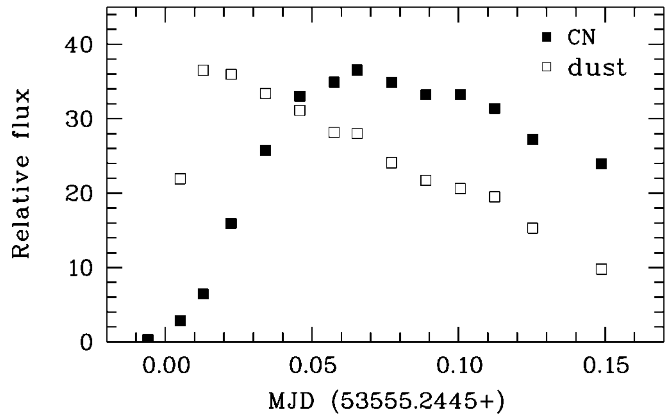

FIG. 2.—HIRES CN and dust impact light curves. Time 0.0 is the time of the impact as observed from Earth: MJD 53,555.2445 (July 4, UT 05:52:02). Each data point represents for each spectrum (at mid-exposure) the total (spatially integrated) flux in the CN (0–0) violet band (388 nm) and in the dust continuum underlying the CN features (*open and filled squares, respectively*). The fluxes are normalized to the exposure time, corrected for air mass, and the respective backgrounds are subtracted. The CN curve is scaled (× 3.5) to the dust curve for easier comparison.

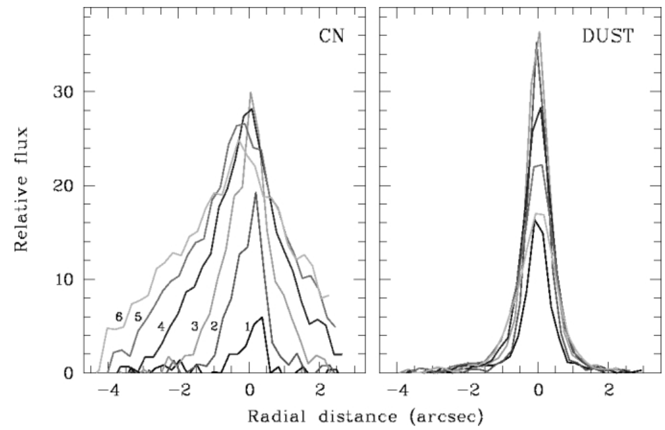

FIG. 3.—HIRES CN and dust radial profiles during the first hour following the impact. The profiles of the first six postimpact spectra (respectively, at mid-exposure time 06:00:18.0, 06:11:12.0, 06:24:35.0, 06:40:29.0, 06:56:22.0, and 07:12:16.0 UT, July 4) are extracted along the 7″ slit of the spectrograph and background-subtracted. The pixel scale in the spatial direction is 0″.239 or 155 km. The slit was set along the parallactic angle with the consequence that the position angle (P.A.) on sky was changing during the observations (20°.1, 24°.8, 29°.7, 35°.5, 40°.6, and 48°.9 for, respectively, the first six postimpact spectra). This direction is close to the axis of the expanding cloud (P.A. = 225°; A'Hearn et al. 2005). Note that the P.A. of the extended Sun-comet radius vector is 111°. The profiles are recentered on the dust peak to compensate for the shift along the slit induced by the atmospheric refraction. The different behavior of the gas and the dust is obvious. [*See the electronic edition of the Journal for a color version of this figure.*]

of the CN parent is indeed long enough [Rauer et al. 2003] to make the escape from the slit width unnoticeable). The average projected speed for CN to cross the half-slit is then ∼0.40 ± 0.04 km s^{-1}. This is smaller than typical molecular outflow velocities in cometary comae (Combi et al. 2005), but it is only a lower limit due to the projection effect. The CN peak intensity of the spatial profiles is reached well before the total CN flux maximum, at about UT 06:30 (±10 minutes).

The CN light curve contains valuable information about the dissociation lifetime of its parent molecule, but a complete modeling is beyond the scope of this Letter. To first approximation, the CN impact light curve may be interpreted by assuming a competition between the CN creation resulting from the dissociation of a parent molecule ($\propto [1 - \exp(-t/\tau)]$, where τ is the parent lifetime) and the exit from the slit area ($\propto t^{-1}$ after filling the slit width and t^{-2} after filling the slit length). A precise determination of the parent lifetime from our data would require a good knowledge of the CN velocity distribution. The radial profiles (Fig. 3) indicate a range of projected velocities from 250 to 650 m s^{-1}, in good agreement with the mean velocity of 400 m s^{-1} deduced from the light curve. Adopting 400 m s^{-1}, the slow decline of the light curve indicates that CN creation still occurs after filling the slit area, requiring relatively long parent lifetimes in agreement with those determined using the *Rosetta* spacecraft data ($\tau \sim 50{,}000$ s; Keller et al. 2005).

The excess of the CN flux observed with UVES until 2 days after the impact indicates that the decline might have occurred in two phases, a fast one documented by HIRES and a slow one lasting over more than a full rotation of the comet. A linear extrapolation of the flux decrease observed by HIRES after the impact shows that the extra CN should have been gone from the area studied about 8 hr after the impact. The excess measured in UVES data could be explained by remnant activity of the crater or the presence of another minor CN parent with a longer lifetime. Unfortunately, data are missing to describe the light curve between MJD 53,555.4 and 53,556.0.

Taking the observed time evolution of the CN excess during the impact as the response of the comet to an elementary event, we tried to model the out-of-impact CN light curve as the response to a series of such elementary pulses. The observations can be accurately reproduced with just three bursts (or jets, corresponding to the observed bumps; see Fig.1). These are simulated by convolving the elementary response with a simple temporal variation representing the instantaneous production of each source. There is no room for a "background" CN flux; i.e., all the CN is produced by these periodic jets starting to release gas at phases 0.25, 0.45, and 0.85 (with an intensity of, respectively, 0.2, 0.7, and 1.0). The FWHM duration of the bursts is 8 hr assuming a quasi-symmetrical triangular shape to the intensity of the jets. This behavior equally explains NH and presumably all gases.

The variations of the dust after the impact are much faster, with a very steep brightening. The maximum is already reached at about UT 06:18 ± 10 minutes, the dust being at that time enhanced by a factor of ∼8.5 with respect to the preimpact spectrum. Contrary to CN, the intensity peak in the dust profiles is reached at about the same time as the spatially integrated flux. The decline of the dust emission may also be interpreted by the escape of dust from the slit. This would give a projected dust velocity of ∼0.18 ± 0.05 km s^{-1}, as, in this case, the escape from the slit width will be the dominant factor. However, the slow and quasi-linear decline would require a rather broad range of velocities—slower than the gas component (Fig. 3)—and/or complex processes like the destruction of highly reflective icy grains by sunlight. The radial profiles show that the dust is expanding at a much slower pace than CN, at about 0.13 ± 0.03 km s^{-1} during the first 1.5 hr after the impact. This is consistent with the value given above and with what others have measured (Keller et al. 2005; Sugita et al. 2005).

There is a slight but clear increasing shift of the position of the CN intensity peak in the radial profiles with respect to the dust (nucleus-dominated) peak (Fig. 3). The shift of ∼350 km (at 07:10 UT, and at a mean P.A. = 215°) is in the direction of the plume ejecta and is most certainly associated with it. It may indicate a preferential ejection direction for the gas with respect to the dust, with the gas being emitted toward the Sun.

4. ISOTOPIC RATIOS

Measuring the isotopic ratios in 9P/Tempel 1 before and after the impact was a unique opportunity to check whether or not the material buried several meters below the surface and released by the impact is different from what we usually observe.

It was important to obtain a high-quality preimpact spectrum in order to compare it with postimpact data. This was achieved with UVES thanks to the 10 hr obtained in June and the 8 hr obtained during the two preimpact nights. The individual CN (0–0) violet band spectra were combined after extraction with an optimal weighting scheme in order to maximize the overall signal-to-noise ratio. Synthetic spectra of the different CN isotopes were computed for each observing circumstance following the scheme described by Zucconi & Festou (1985). The isotope mixture was then adjusted to best fit the observed final spectrum (Arpigny et al. 2003; Jehin et al. 2004). The same was done for the UVES postimpact data, and since no difference was found (which is not too surprising since those spectra were only slightly affected by the impact [Fig. 1]), all the spectra were combined to produce a single 50 hr spectrum. The best fit is obtained for an isotopic mixture $^{12}C/^{13}C = 95 \pm 15$ and $^{14}N/^{15}N = 145 \pm 20$.

From the HIRES impact light curve (Fig. 2), we extracted the spectra showing a brightening of more than a factor of 2 (the 10 spectra from 06:33 to 09:11 UT). Thus, in those spectra, half the CN flux might come from the fresh material released by the impactor. Despite the shorter exposure time (about 4 hr of total exposure time) and the lower resolving power of the HIRES spectrum compared to the UVES out-of-impact spectrum, the large collecting area of the Keck I telescope and the relative brightening of the comet allowed us to determine the following values: $^{12}C/^{13}C = 95 \pm 15$ and $^{14}N/^{15}N = 165 \pm 30$ for the carbon and nitrogen isotopic ratios. Those values are compatible with the values determined out of impact. It appears that the $^{14}N/^{15}N$ ratio of the buried material is still most probably below the solar value (Arpigny et al. 2003).

After comet 88P/Howell, comet 9P/Tempel 1 is the second Jupiter-family comet to have a $^{14}N/^{15}N$ ratio determination. Both values are in excellent agreement and are similar to the ratios measured in half a dozen Oort-cloud comets (Hutsemékers et al. 2005). The fact that the ejected material—supposed to be pristine since it was never exposed to the solar radiation and cosmic rays—has the same isotopic composition favors an isotopic homogeneity between the two populations of comets, despite the fact that they are expected to have formed at very different locations in the solar system (Weissman 1999). This is a strong argument in favor of a primordial origin for the high content of ^{15}N in cometary volatiles. This peculiarity is not the result of some alteration process of the comet's surface material and was already present in the protosolar nebula before the accretion process, which gave birth to the comets and planets, took place. In case the N isotopic ratio changes within the solar nebula, this is a new argument in favor of the volatile ices in Jupiter-family and Oort-cloud comets originating in a common region of the protoplanetary disk (Mumma et al. 2005).

The work in this Letter is based on observations carried out at the European Southern Observatory (ESO) under program 075.C-0355(A). This program was part of a joint European initiative in support of the NASA *Deep Impact* mission to comet 9P/Tempel 1 by ground-based observations at La Silla and VLT Paranal. Some of the material presented herein is based on data obtained at the W. M. Keck Observatory, which immediately made its data available to the public after impact occurred on 2005 July 4. The W. M. Keck Observatory is operated as a scientific partnership among the California Institute of Technology, the University of California, and the National Aeronautics and Space Administration. The Observatory was made possible by the generous financial support of the W. M. Keck Foundation. The authors wish to recognize and acknowledge the very significant cultural role and reverence that the summit of Mauna Kea has always had within the indigenous Hawaiian community. We are most fortunate to have the opportunity to get observations from this mountain. J. M. is Research Director, and D. H. is Research Associate, at FNRS (Belgium).

REFERENCES

A'Hearn, M. F., et al. 2005, Science, 310, 258
Arpigny, C., Jehin, E., Manfroid, J., Hutsemékers, D., Schulz, R., Stüwe, J. A., Zucconi, J.-M., & Ilyin, I. 2003, Science, 301, 1522
Biver, N., Bockelée-Morvan, D., Colom, P., Crovisier, J., Lecacheux, A., & Paubert, G. 2005, IAU Circ. 8538
Combi, M. R., Harris, W. M., & Smyth, W. H. 2005, in Comets II, ed. M. C. Festou, H. U. Keller, & H. A. Weaver (Tucson: Univ. Arizona Press), 523
Fink, U., Combi, M. R., & DiSanti, M. A. 1991, ApJ, 383, 356
Fray, N., Bénilan, Y., Cottin, H., Gazeau, M.-C., & Crovisier, J. 2005, Planet. Space Sci., 53, 1243
Hutsemékers, D., Manfroid, J., Jehin, E., Arpigny, C., Cochran, A., Schulz, R., Stüwe, J. A., & Zucconi, J.-M. 2005, A&A, 440, L21
Jehin, E., et al. 2004, ApJ, 613, L161
Keller, H., et al. 2005, Science, 310, 281
Manfroid, J., Jehin, E., Hutsemékers, D., Cochran, A., Zucconi, J.-M., Arpigny, C., Schulz, R., & Stüwe, J. A. 2005, A&A, 432, L5
Mumma, M. J., et al. 2005, Science, 310, 270
Rauer, H., et al. 2003, A&A, 397, 1109
Renson, P. 1978, A&A, 63, 125
Schleicher, D. G., et al. 1990, AJ, 100, 896
Sugita, S., et al. 2005, Science, 310, 274
Weissman, P. R. 1999, Space Sci. Rev., 90, 301
Wyckoff, S., Tegler, S., Wehinger, P. A., Spinrad, H., & Belton, M. J. S. 1988, ApJ, 325, 927
Zucconi, J. M., & Festou, M. C. 1985, A&A, 150, 180